2

Available Solar Radiation

In this chapter we describe instruments for solar radiation measurements, the solar radiation data that are available, and the calculation of needed information from the available data. It is generally not practical to base predictions or calculations of solar radiation on attenuation of the extraterrestrial radiation by the atmosphere, as adequate meteorological information is seldom available. Instead, to predict the performance of a solar process in the future, we use past measurements of solar radiation at the location in question or from a nearby similar location.

Solar radiation data are used in several forms and for a variety of purposes. The most detailed information available is beam and diffuse solar radiation on a horizontal surface, by hours, which is useful in simulations of solar processes. (A few measurements are available on inclined surfaces and for shorter time intervals.) Daily data are often available and hourly radiation can be estimated from daily data. Monthly total solar radiation on a horizontal surface can be used in some process design methods. However, as process performance is generally not linear with solar radiation, the use of averages may lead to serious errors if nonlinearities are not taken into account. It is also possible to reduce radiation data to more manageable forms by statistical methods.

2.1 DEFINITIONS

Figure 2.1.1 shows the primary radiation fluxes on a surface at or near the ground that are important in connection with solar thermal processes. It is convenient to consider radiation in two wavelength ranges.[1]

Solar or **short-wave radiation** is radiation originating from the sun, in the wavelength range of 0.3 to 3 μm. In the terminology used throughout this book, solar radiation includes both beam and diffuse components unless otherwise specified.

Long-wave radiation is radiation originating from sources at temperatures near ordinary ambient temperatures and thus substantially all at wavelengths greater than 3 μm. Long-wave radiation is emitted by the atmosphere, by a collector, or by any other body

[1] We will see in Chapters 3, 4, and 6 that the wavelength ranges of incoming solar radiation and emitted radiation from flat-plate solar collectors overlap to a negligible extent, and for many purposes the distinction noted here is very useful. For collectors operating at high enough temperatures there is significant overlap and more precise distinctions are needed.

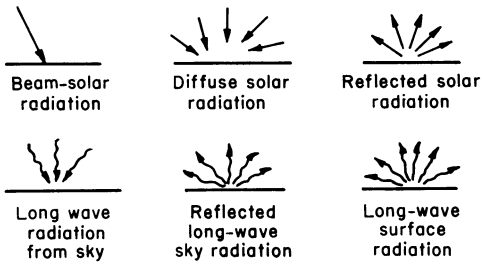

Figure 2.1.1 The radiant energy fluxes of importance in solar thermal processes. Short-wave solar radiation is shown by →. Long-wave radiation is shown by ⇝.

at ordinary temperatures. (This radiation, if originating from the ground, is referred to in some literature as ''terrestrial'' radiation.)

Instruments for measuring solar radiation are of two basic types:

A **pyrheliometer** is an instrument using a collimated detector for measuring solar radiation from the sun and from a small portion of the sky around the sun (i.e., beam radiation) at normal incidence.

A **pyranometer** is an instrument for measuring total hemispherical solar (beam plus diffuse) radiation, usually on a horizontal surface. If shaded from the beam radiation by a shade ring or disc, a pyranometer measures diffuse radiation.

In addition, the terms **solarimeter** and **actinometer** are encountered; a solarimeter can generally be interpreted to mean the same as a pyranometer, and an actinometer usually refers to a pyrheliometer.

In the following sections we discuss briefly the two basic radiation instruments and the pyrheliometric scales that are used in solar radiometry. More detailed discussions of instruments, their use, and the associated terminology are found in Robinson (1966), World Meteorological Organization (WMO, 1969), Kondratyev (1969), Coulson (1975), Thekaekara (1976), Yellott (1977), and Iqbal (1983). Stewart et al. (1985) review characteristics of pyranometers and pyrheliometers.

2.2 PYRHELIOMETERS AND PYRHELIOMETRIC SCALES

Standard and secondary standard solar radiation instruments are pyrheliometers. The water flow pyrheliometer, designed by Abbot in 1905, was an early standard instrument. This instrument uses a cylindrical blackbody cavity to absorb radiation that is admitted through a collimating tube. Water flows around and over the absorbing cavity, and measurements of its temperature and flow rate provide the means for determining the absorbed energy. The design was modified by Abbot in 1932 to include the use of two thermally identical chambers, dividing the cooling water between them and heating one chamber electrically while the other is heated by solar radiation; when the instrument is adjusted so as to make the heat produced in the two chambers identical, the electrical power input is a measure of the solar energy absorbed.

Standard pyrheliometers are not easy to use, and secondary standard instruments have been devised that are calibrated against the standard instruments. The secondary

standards in turn are used to calibrate field instruments. Robinson (1966) and Coulson (1975) provide detailed discussion and bibliography on this topic. Two of these secondary standard instruments are of importance.

The Abbot silver disc pyrheliometer, first built by Abbot in 1902 and modified in 1909 and 1927, uses a silver disc 38 mm in diameter and 7 mm thick as the radiation receiver. The side exposed to radiation is blackened, and the bulb of a precision mercury thermometer is inserted in a hole in the side of the disc and is in good thermal contact with the disc. The silver disc is suspended on wires at the end of a collimating tube, which in later models has dimensions such that 0.0013 of the hemisphere is ''seen'' by the detector. Thus any point on the detector sees an aperture angle of 5.7°. The disc is mounted in a copper cylinder, which in turn is in a cylindrical wood box that insulates the copper and the disc from the surroundings. A shutter alternately admits radiation and shades the detector at regular intervals; the corresponding changes in disc temperature are measured and provide the means to calculate the absorbed radiation. A section drawing of the pyrheliometer is shown is Figure 2.2.1.

The other secondary standard of particular importance is the Ångström compensation pyrheliometer, first constructed by K. Ångström in 1893 and modified in several developments since then. In this instrument two identical blackened manganin strips are arranged so that either one can be exposed to radiation at the base of collimating tubes by moving a reversible shutter. Each strip can be electrically heated, and each is fitted with a thermocouple. With one strip shaded and one strip exposed to radiation, a current is passed through the shaded strip to heat it to the same temperature as the exposed strip. When there is no difference in temperature, the electrical energy to the shaded strip must equal the solar radiation absorbed by the exposed strip. Solar radiation is determined by equating the electrical energy to the product of incident solar radiation, strip area, and absorptance. After a determination is made, the position of the shutter is reversed to

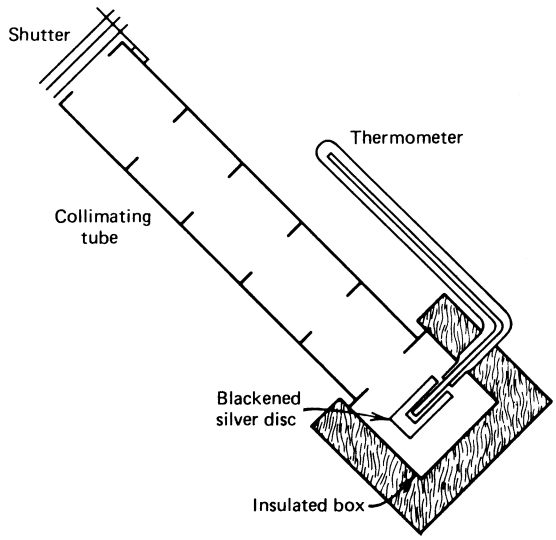

Figure 2.2.1 Schematic section of the Abbot silver disc pyrheliometer.

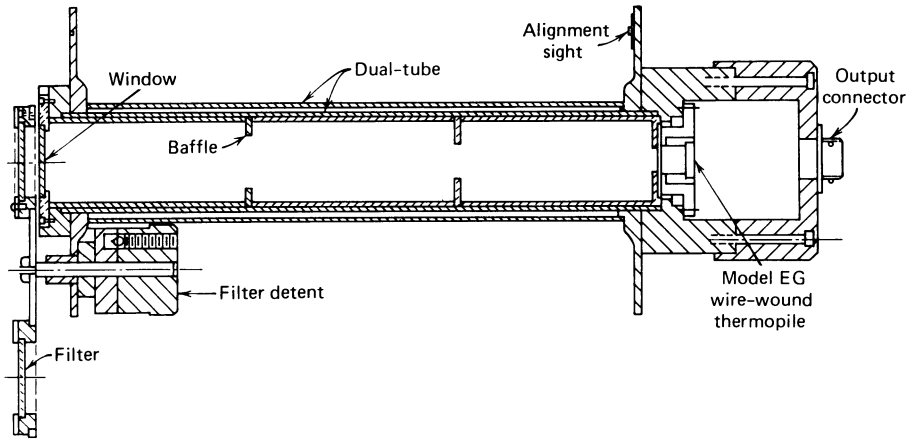

Figure 2.2.2 Cross section of the Eppley NIP. Courtesy of The Eppley Laboratory.

The dimensions of the collimating systems are such that the detectors are exposed to radiation from the sun and from a portion of the sky around the sun. Since the detectors do not distinguish between forward-scattered radiation, which comes from the circumsolar sky, and beam radiation, the instruments are, in effect, defining beam radiation. An experimental study by Jeys and Vant-Hull (1976) which utilized several lengths of collimating tubes so that the aperture angles were reduced in step from 5.72° to 2.02° indicated that for cloudless conditions this reduction in aperture angle resulted in insignificant changes in the measurements of beam radiation. On a day of thin uniform cloud cover, however, with solar altitude angle of less than 32°, as much as 11% of the measured

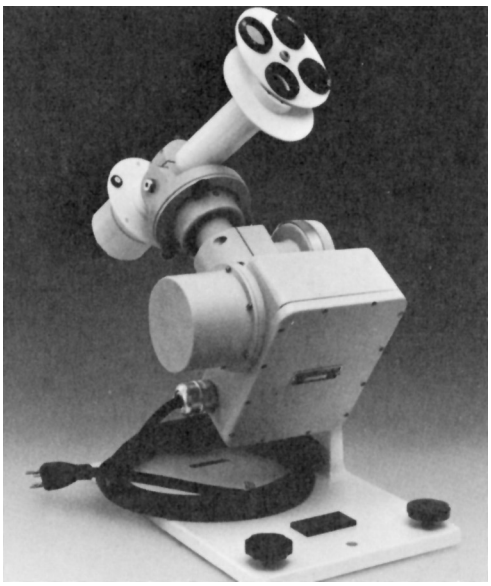

Figure 2.2.3 An Eppley NIP on an altazimuth tracking mount. Courtesy of The Eppley Laboratory.

$$\phi = \begin{cases} 0 & \text{if } X_c \geq X_m \\ \left(1 - \dfrac{X_c}{X_m}\right)^2 & \text{if } X_m = 2 \\ \left|g - \left[g^2 + (1 + 2g)\left(1 - \dfrac{X_c}{X_m}\right)^2\right]^{1/2}\right| & \text{otherwise} \end{cases} \tag{2.23.5a}$$

where

$$g = \frac{X_m - 1}{2 - X_m} \tag{2.23.5b}$$

$$X_m = 1.85 + 0.169\,\frac{\overline{R}_h}{\overline{k}_T^2} + 0.0696\,\frac{\cos\beta}{\overline{k}_T^2} - 0.981\,\frac{\overline{k}_T}{\cos^2\delta} \tag{2.23.5c}$$

The monthly average hourly clearness index $\overline{k}_T$ is defined as

$$\overline{k}_T = \frac{\overline{I}}{I_o} \tag{2.23.6}$$

It can be estimated using Equations 2.13.2 and 2.13.4:

$$\overline{k}_T = \frac{\overline{I}}{\overline{I}_o} = \frac{r_t}{r_d}\frac{\overline{H}}{\overline{H}_o} = \frac{r_t}{r_d}\overline{K}_T = (a + b\cos\omega)\,\overline{K}_T \tag{2.23.7}$$

where a and b are given by Equations 2.13.2b and 2.13.2c.

The remaining term in Equation 2.23.5 is $\overline{R}_h$, the ratio of monthly average hourly radiation on the tilted surface to that on a horizontal surface:

$$\overline{R}_h = \frac{\overline{I}_T}{\overline{I}} = \frac{\overline{I}_T}{r_T\overline{H}} \tag{2.23.8}$$

Example 2.23.3

Repeat Example 2.23.2 using the Clark et al. equations.

Solution

The calculations to be made are $\overline{R}_h$, $\overline{k}_T$, X_m, X_c, g, and finally ϕ. Intermediate results from Example 2.23.2 that are useful here are $\overline{I}_T = 2.33$ MJ/m^2, $r_t = 0.158$, $\omega_s = 78.9°$, $\omega = 7.5°$, and $X_c = 0.549$:

$$\overline{R}_h = \frac{\overline{I}_T}{\overline{I}} = \frac{\overline{I}_T}{r_t\overline{H}} = \frac{2.33}{1.58 \times 20.3 \times 0.50} = 1.44$$

To calculate $\overline{k}_T$, we need the constants a and b in Equation 2.23.7:

$$a = 0.409 + 0.5016 \sin(78.9 - 60) = 0.571$$

$$b = 0.6609 - 0.4767 \sin(78.9 - 60) = 0.506$$

Thus

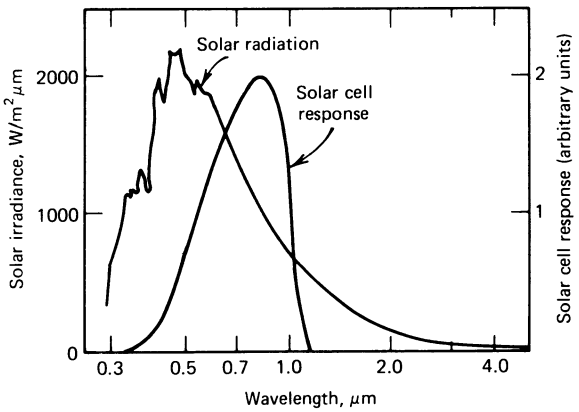

Figure 2.3.3 Spectral distribution of extraterrestrial solar radiation and spectral response of a silicon solar cell. From Coulson, (1975).

Photovoltaic detectors have additional characteristics of interest. Their response to changing radiation levels is essentially instantaneous and is linear with radiation. The temperature dependence is $\pm 0.15\%/°C$ maximum. The LI-COR instrument is fitted with an acrylic diffuser that substantially removes the dependence of response on the angle of incidence of the radiation. The response of the detectors is independent of its orientation, but reflected radiation from the ground or other surroundings will in general have a different spectral distribution than global horizontal radiation, and measurements on surfaces receiving significant amounts of reflected radiation will be subject to additional errors.

The preceding discussion dealt entirely with measurements of total radiation on a horizontal surface. Two additional kinds of measurements are made with pyranometers: measurements of diffuse radiation on horizontal surfaces and measurements of solar radiation on inclined surfaces.

Measurements of diffuse radiation can be made with pyranometers by shading the instrument from beam radiation. This is usually done by means of a shading ring, as shown in Figure 2.3.4. The ring is used to allow continuous recording of diffuse radiation without the necessity of continuous positioning of smaller shading devices; adjustments need to be made for changing declination only and can be made every few days. The ring shades the pyranometer from part of the diffuse radiation, and a correction for this shading must be estimated and applied to the observed diffuse radiation (Drummond, 1956, 1964; IGY, 1958; Coulson, 1975). The corrections are based on assumptions of the distribution of diffuse radiation over the sky and typically are factors of 1.05 to 1.2. An example of shade ring correction factors, to illustrate their trends and magnitudes, is shown in Figure 2.3.5.

Measurements of solar radiation on inclined planes are important in determining the input to solar collectors. There is evidence that the calibration of pyranometers changes if the instrument is inclined to the horizontal. The reason for this appears to be changes in the convection patterns inside the glass dome, which changes the manner in which heat is transferred from the hot junctions of the thermopiles to the cover and other parts of the instrument. The Eppley 180° pyranometer has been variously reported to show a

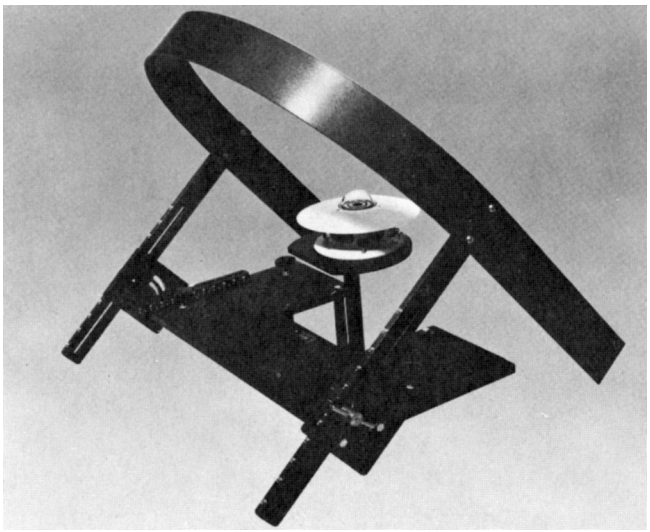

Figure 2.3.4 Pyranometer with shading ring to eliminate beam radiation. Courtesy of The Eppley Laboratory.

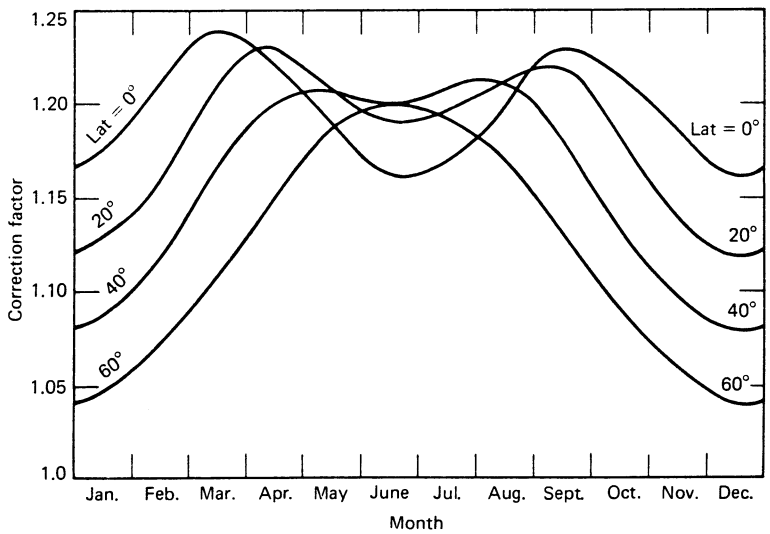

Figure 2.3.5 Typical shade ring correction factors to account for shading of the detector from diffuse radiation. Adapted from Coulson (1975).

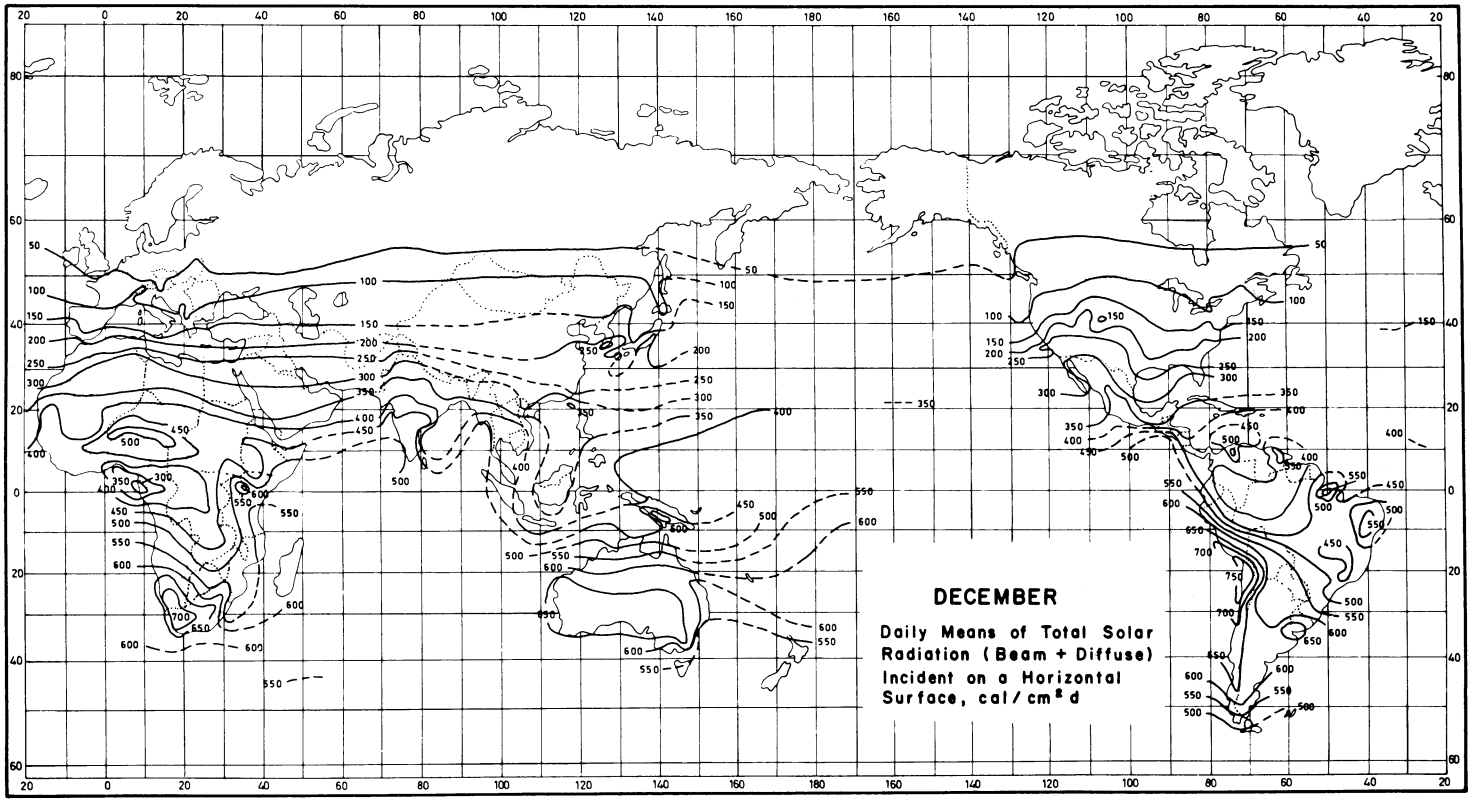

Figure 2.5.2 Average daily radiation on horizontal surfaces for December. Data are in cal/cm^2, the traditional units. Adapted from deJong (1973) and Löf et al. (1966a).

Table 2.5.1 Hourly Radiation for Hour Ending at Indicated Time, Air Temperature, and Wind Speed Data for January Week, Boulder, Colorado

Day	Hour	I (kJ/m^2)	T_a (°C)	V (m/s)	Day	Hour	I (kJ/m^2)	T_a (°C)	V (m/s)
8	1	0	−1.7	3.1	8	13	1105	2.8	8.0
8	2	0	−3.3	3.1	8	14	1252	3.8	9.8
8	3	0	−2.8	3.1	8	15	641	3.3	9.8
8	4	0	−2.2	3.1	8	16	167	2.2	7.2
8	5	0	−2.8	4.0	8	17	46	0.6	7.6
8	6	0	−2.8	3.6	8	18	0	−0.6	7.2
8	7	0	−2.2	3.6	8	19	0	−1.1	8.0
8	8	17	−2.2	4.0	8	20	0	−1.7	5.8
8	9	134	−1.1	1.8	8	21	0	−1.7	5.8
8	10	331	1.1	3.6	8	22	0	−2.2	7.2
8	11	636	2.2	1.3	8	23	0	−2.2	6.3
8	12	758	2.8	2.2	8	24	0	−2.2	5.8
9	1	0	−2.8	7.2	9	13	1185	−2.2	2.2
9	2	0	−3.3	7.2	9	14	1009	−1.3	1.7
9	3	0	−3.3	6.3	9	15	796	−0.6	1.3
9	4	0	−3.3	5.8	9	16	389	−0.6	1.3
9	5	0	−3.9	4.0	9	17	134	−2.2	4.0
9	6	0	−3.9	4.5	9	18	0	−2.8	4.0
9	7	0	−3.9	1.8	9	19	0	−3.3	4.5
9	8	4	−3.9	2.2	9	20	0	−5.6	5.8
9	9	71	−3.9	2.2	9	21	0	−6.7	5.4
9	10	155	−3.3	4.0	9	22	0	−7.8	5.8
9	11	343	−2.8	4.0	9	23	0	−8.3	4.5
9	12	402	−2.2	4.0	9	24	0	−8.3	6.3
10	1	0	−9.4	5.8	10	13	1872	2.2	7.6
10	2	0	−10.0	6.3	10	14	1733	4.4	6.7
10	3	0	−8.9	5.8	10	15	1352	6.1	6.3
10	4	0	−10.6	6.3	10	16	775	6.7	4.0
10	5	0	−8.3	4.9	10	17	205	6.1	2.2
10	6	0	−8.3	7.2	10	18	4	3.3	4.5
10	7	0	−10.0	5.8	10	19	0	0.6	4.0
10	8	33	−8.9	5.8	10	20	0	0.6	3.1
10	9	419	−7.2	6.7	10	21	0	0.0	2.7
10	10	1047	−5.0	9.4	10	22	0	0.6	2.2
10	11	1570	−2.2	8.5	10	23	0	1.7	3.6
10	12	1805	−1.1	8.0	10	24	0	0.6	2.7
11	1	0	−1.7	8.9	11	13	138	−5.0	6.7
11	2	0	−2.2	4.9	11	14	96	−3.9	6.7
11	3	0	−2.2	4.5	11	15	84	−4.4	7.6
11	4	0	−2.8	5.8	11	16	42	−3.9	6.3
11	5	0	−4.4	5.4	11	17	4	−5.0	6.3
11	6	0	−5.0	4.5	11	18	0	−5.6	4.5

where β is the Ångström turbidity coefficient, α is a single lumped wavelength exponent, λ is the wavelength in micrometers, and m is the air mass along the path of interest. Thus there are two parameters, β and α, that describe the atmospheric turbidity and its wavelength dependence; β varies from 0 to 0.4 for very clean to very turbid atmospheres, α depends on the size distribution of the aerosols (a value of 1.3 is commonly used). Both β and α vary with time as atmospheric conditions change.

More detailed discussions of scattering are provided by Fritz (1958), who included effects of clouds, by Thekaekara (1974) in a review, and by Iqbal (1983).

Absorption of radiation in the atmosphere in the solar energy spectrum is due largely to ozone in the ultraviolet and to water vapor and carbon dioxide in bands in the infrared. There is almost complete absorption of short-wave radiation by ozone in the upper atmosphere at wavelengths below 0.29 μm. Ozone absorption decreases as λ increases above 0.29 μm, until at 0.35 μm there is no absorption. There is also a weak ozone absorption band near $\lambda = 0.6$ μm.

Water vapor absorbs strongly in bands in the infrared part of the solar spectrum, with strong absorption bands centered at 1.0, 1.4, and 1.8 μm. Beyond 2.5 μm, the transmission of the atmosphere is very low due to absorption by H_2O and CO_2. The energy in the extraterrestrial spectrum at $l > 2.5$ μm is less than 5% of the total solar spectrum, and energy received at the ground at $\lambda > 2.5$ μm is very small.

The effects of Rayleigh scattering by air molecules and absorption by O_3, H_2O, and CO_2 on the spectral distribution of beam irradiance are shown in Figure 2.6.1 for an atmosphere with $b = 0$ and 2 cm of precipitable water, w. The WRC extraterrestrial distribution is shown as a reference. The Rayleigh scattering is represented by the difference between the extraterrestrial curve and the curve at the top of the shaded areas; its effect becomes small at wavelengths greater than about 0.7 μm. The several absorption bands are shown by the shaded areas.

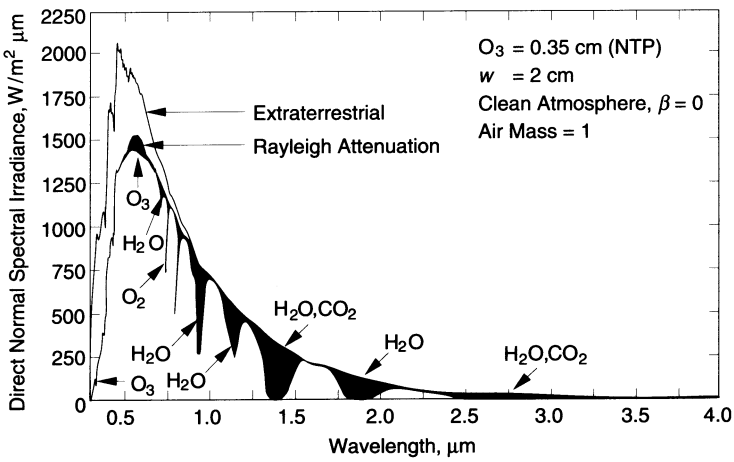

Figure 2.6.1 An example of the effects of Raleigh scattering and atmospheric absorption on the spectral distribution of beam irradiance. Adapted from Iqbal (1983).

Table 2.6.1 Spectral Distribution of Terrestrial Beam Normal Radiation at Air Mass 1.5, Precipitable Water 1.42 cm, O_3 = 0.34 atm-cm, CO_2 = 370 ppm, in Equal Increments of Energy[a]

Energy Band $f_i - f_{i+1}$	Wavelength Range (μm)	Midpoint-Wavelength (μm)
0.00–0.05	0.280–0.426	0.396
0.05–0.10	0.426–0.470	0.451
0.10–0.15	0.470–0.508	0.490
0.15–0.20	0.508–0.545	0.527
0.20–0.25	0.545–0.581	0.563
0.25–0.30	0.581–0.617	0.599
0.30–0.35	0.617–0.653	0.635
0.35–0.40	0.653–0.691	0.672
0.40–0.45	0.691–0.732	0.710
0.45–0.50	0.732–0.777	0.752
0.50–0.55	0.777–0.822	0.798
0.55–0.60	0.822–0.871	0.846
0.60–0.65	0.871–0.929	0.896
0.65–0.70	0.929–1.012	0.981
0.70–0.75	1.012–1.080	1.044
0.75–0.80	1.080–1.201	1.142
0.80–0.85	1.201–1.300	1.249
0.85–0.90	1.300–1.588	1.510
0.90–0.95	1.588–1.974	1.678
0.95–1.00	1.974–5.000	2.232

[a]From SMARTS.

In summary, the normal solar radiation incident on the earth's atmosphere has a spectral distribution indicated by Figure 1.3.1. The x-rays and other very short wave radiation of the solar spectrum are absorbed high in the ionosphere by nitrogen, oxygen, and other atmospheric components. Most of the ultraviolet is absorbed by ozone. At wavelengths longer than 2.5 μm, a combination of low extraterrestrial radiation and strong absorption by CO_2 means that very little energy reaches the ground. Thus, from the viewpoint of terrestrial applications of solar energy, only radiation of wavelengths between 0.29 and 2.5 μm need be considered.

2.7 ESTIMATION OF AVERAGE SOLAR RADIATION

Radiation data are the best source of information for estimating average incident radiation. Lacking these or data from nearby locations of similar climate, it is possible to use empirical relationships to estimate radiation from hours of sunshine or cloudiness. Data on average hours of sunshine or average percentage of possible sunshine hours are widely

available from many hundreds of stations in many countries and are usually based on data taken with Campbell-Stokes instruments. Examples are shown in Table 2.7.1. Cloud cover data (i.e., cloudiness) are also widely available but are based on visual estimates and are probably less useful than hours of sunshine data.

The original Ångström-type regression equation related monthly average daily radiation to clear-day radiation at the location in question and average fraction of possible sunshine hours:

$$\frac{\overline{H}}{\overline{H}_c} = a' + b' \frac{\overline{n}}{\overline{N}} \tag{2.7.1}$$

where $\overline{H}$ = monthly average daily radiation on horizontal surface
$\overline{H}_c$ = average clear-sky daily radiation for location and month in question
a', b' = empirical constants
$\overline{n}$ = monthly average daily hours of bright sunshine
$\overline{N}$ = monthly average of maximum possible daily hours of bright sunshine (i.e., day length of average day of month)

A basic difficulty with Equation 2.7.1 lies in the ambiguity of the terms $\overline{n}/\overline{N}$ and $\overline{H}_c$. The former is an instrumental problem (records from sunshine recorders are open to interpretation). The latter stems from uncertainty in the definition of a clear day. Page (1964) and others have modified the method to base it on extraterrestrial radiation on a horizontal surface rather than on clear-day radiation:

$$\frac{\overline{H}}{\overline{H}_o} = a + b \frac{\overline{n}}{\overline{N}} \tag{2.7.2}$$

Table 2.7.1 Examples of Monthly Average Hours per Day of Sunshine by Latitude and Altitude

Location Latitude Altitude, m	Hong Kong, 22° N, Sea Level	Paris, France, 48° N, 50 m	Bombay, India, 19° N, Sea Level	Sokoto, Nigeria, 13° N, 107 m	Perth, Australia, 32° S, 20 m	Madison, Wisconsin, 43° N, 270 m
January	4.7	2.1	9.0	9.9	10.4	4.5
February	3.5	2.8	9.3	9.6	9.8	5.7
March	3.1	4.9	9.0	8.8	8.8	6.9
April	3.8	7.4	9.1	8.9	7.5	7.5
May	5.0	7.1	9.3	8.4	5.7	9.1
June	5.3	7.6	5.0	9.5	4.8	10.1
July	6.7	8.0	3.1	7.0	5.4	9.8
August	6.4	6.8	2.5	6.0	6.0	10.0
September	6.6	5.6	5.4	7.9	7.2	8.6
October	6.8	4.5	7.7	9.6	8.1	7.2
November	6.4	2.3	9.7	10.0	9.6	4.2
December	5.6	1.6	9.6	9.8	10.4	3.9
Annual	5.3	5.1	7.4	8.8	7.8	7.3